

# Parametric investigation of miniaturized cylindrical and annular Hall thrusters

A. Smirnov,<sup>a)</sup> Y. Raitses, and N. J. Fisch

*Princeton University Plasma Physics Laboratory, P.O. Box 451, Princeton, New Jersey 08543*

(Received 22 May 2002; accepted 23 August 2002)

Conventional annular Hall thrusters become inefficient when scaled to low power. An alternative approach, a 2.6 cm miniaturized cylindrical Hall thruster with a cusp-type magnetic field distribution, was developed and studied. Its performance was compared to that of a conventional annular thruster of the same dimensions. The cylindrical thruster exhibits discharge characteristics similar to those of the annular thruster, but it has a much higher propellant ionization efficiency. Significantly, a large fraction of multicharged xenon ions might be present in the outgoing ion flux generated by the cylindrical thruster. The operation of the cylindrical thruster is quieter than that of the annular thruster. The characteristic peak in the discharge current fluctuation spectrum at 50–60 kHz appears to be due to ionization instabilities. In the power range 50–300 W, the cylindrical and annular thrusters have comparable efficiencies (15%–32%) and thrusts (2.5–12 mN). For the annular configuration, a voltage less than 200 V was not sufficient to sustain the discharge at low propellant flow rates. The cylindrical thruster can operate at voltages lower than 200 V, which suggests that a cylindrical thruster can be designed to operate at even smaller power. © 2002 American Institute of Physics. [DOI: 10.1063/1.1515106]

## I. INTRODUCTION

Low-power propulsion devices, with small spacecraft mass, might enable new scientific and exploration space missions, such as multiple microspacecraft flying in constellations.<sup>1,2</sup> The Hall thruster is a mature electric propulsion device at intermediate to high power, but it appears to be promising also for relatively low-power primary propulsion on near-Earth missions,<sup>3</sup> such as orbit transfer and repositioning. At even lower power and smaller sizes, the cylindrical Hall thruster that we explore here may have advantages over the conventional annular Hall thruster.

In a conventional Hall thruster,<sup>4</sup> the axial electric and radial magnetic fields are applied in an annular channel. The magnetic field is large enough to lock the electrons in the azimuthal  $E \times B$  drift, but small enough to leave the ion trajectories almost unaffected. The thrust is generated in reaction to the axial electrostatic acceleration of ions. Ions are accelerated in a quasineutral plasma, so that no space-charge limitation is imposed on the achievable current and thrust densities. Conventional Hall thrusters designed for operation in 600–1000 W power range have an outer channel diameter about 10 cm, maximal value of the magnetic field radial component about 100 G, and applied discharge voltage  $U_d = 300$  V. The thruster efficiency, defined as a ratio of the kinetic energy flux at the thruster exit to the input electrical power, is about 50%–60%. Typical values of plasma parameters in a conventional Hall thruster are the following: Electron density  $n_e \sim 10^{11} - 10^{12}$  cm<sup>-3</sup>, electron temperature  $T_e \sim 10 - 20$  eV, ion temperature  $T_i \sim 1$  eV, and ion exhaust velocity  $V_i \sim 16\,000$  m/s.

A smaller operating power of a Hall thruster implies either smaller discharge voltage or smaller discharge current. The degree to which the first option can be accommodated is limited by the necessity to keep the exhaust ion velocity high. The second option implies that the propellant flow rate should be decreased. In order to maintain high propellant utilization efficiency at low propellant flow rates, the thruster channel must be scaled down to preserve the ionization probability. Thus, according to Ref. 5, the acceleration region length, which is mainly determined by the magnetic field distribution, must be decreased linearly together with the channel sizes, while the magnetic field must be increased inversely to the scaling factor. However, the implementation of the latter requirement is technically challenging because of magnetic saturation in the miniaturized inner parts of the magnetic core. A linear scaling down of the magnetic circuit leaves almost no room for magnetic poles or for heat shields, making difficult the achievement of the optimal magnetic fields. Nonoptimal magnetic fields result in enhanced power and ion losses, heating and erosion of the thruster parts, particularly the critical inner parts of the coaxial channel and magnetic circuit.

Currently existing low-power Hall thruster laboratory prototypes with channel diameters 2–4 cm operate at 100–300 W power levels with efficiencies in the range of 10%–30%.<sup>6–8</sup> However, further scaling of the conventional geometry Hall thruster down to subcentimeter size<sup>9</sup> results in even lower efficiencies (6% at power level of about 100 W). The low efficiency might arise from a large axial electron current, enhanced either by magnetic field degradation due to excessive heating of the thruster magnets or by electron collisions with the channel walls. Thus, miniaturizing the conventional annular Hall thruster does not appear to be straightforward.

<sup>a)</sup>Electronic mail: asmirnov@pppl.gov

The cylindrical Hall thruster suggested in Ref. 10 features a channel with a short annular region and longer cylindrical region, and a cusp-type magnetic field distribution [see Fig. 1(a)]. Having larger volume-to-surface ratio than the conventional annular thruster, and therefore, potentially smaller wall losses in the channel, the cylindrical Hall thruster should suffer lower erosion and heating of the thruster parts. This makes the concept of a cylindrical Hall thruster very promising for low-power applications.

A relatively large 9 cm diameter version of the cylindrical thruster exhibited performance comparable with conventional annular Hall thrusters in the subkilowatt power range.<sup>10</sup> In the present work, we developed and studied a miniature 2.6 cm diameter cylindrical Hall thruster. In order to understand the physics of cylindrical Hall thrusters better and to examine the attractiveness of the cylindrical approach for low-power Hall thruster scaling, we compared the performance of the 2.6 cm cylindrical Hall thruster to that of the conventional annular thruster with the same channel diameter and length. Thruster ac and dc electrical measurements, as well as total ion flux and thrust measurements, were performed. It was found that the cylindrical thruster has unusually high propellant ionization efficiency, compared to conventional Hall thrusters. The ratio of the total ion current to the effective propellant mass flow current, in the case of cylindrical configuration, could exceed unity, which clearly indicates the presence of multicharged Xe ions in the ion flux generated by the thruster. The discharge in the cylindrical thruster was also found to be somewhat quieter than that in the annular thruster: The amplitude of oscillations in the frequency range 10–100 kHz was relatively lower for the cylindrical configuration. However, the spectrum of discharge current oscillations of the cylindrical thruster exhibits a pronounced peak at about 50–60 kHz, which may be due to ionization instabilities.<sup>11</sup> The higher ionization efficiency and quieter operation of the cylindrical thruster suggest that the underlying physics of the cylindrical design may differ significantly from that of the annular design.

This article is organized as follows: In Sec. II, the experimental setup is described. In Sec. III, we describe the experimental results and discuss their implications. In Sec. IV, we summarize our main conclusions.

## II. EXPERIMENTAL SETUP

A 2.6 cm cylindrical Hall thruster shown in Fig. 1 was scaled down from a 9 cm cylindrical Hall thruster to operate at about 200 W power level.<sup>12</sup> Similar to the large thruster, this miniaturized cylindrical thruster consists of a boron-nitride ceramic channel, an annular anode, which serves also as a gas distributor, two electromagnetic coils, and a magnetic core. Field lines of the cusp-type magnetic field intersect the ceramic channel walls. The electron drift trajectories are closed. Magnetic field lines form equipotential surfaces, with  $E = -v_e \times B$ . Ion thrust is generated by the axial component of the Lorentz force, proportional to the radial magnetic field and the azimuthal electron current.

The cylindrical channel features a short annular region, approximately 1 cm long, and a longer cylindrical region.

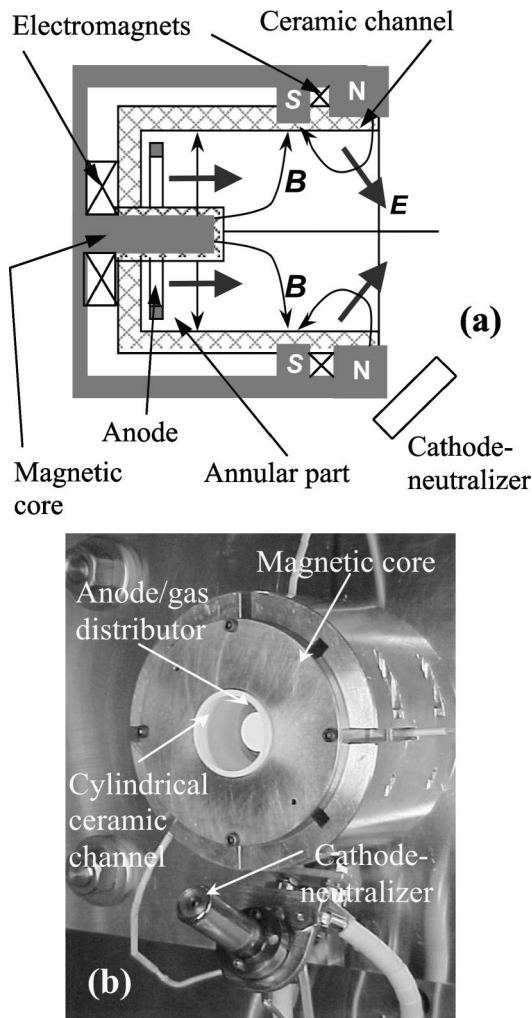


FIG. 1. (a) Schematic of a cylindrical Hall thruster. (b) The 2.6-cm cylindrical Hall thruster.

The total length of the channel is 2.6 cm. The length of the annular region was chosen so as to provide high ionization of the working gas at the boundary of the annular and the cylindrical regions. The outer and the inner diameters of the channel are 2.6 cm and 1.4 cm, respectively.

The thruster design allows one to vary the thruster geometry. By extending the central pole of the magnetic core and the central ceramic piece up to the exit plane of the channel, the cylindrical thruster can be converted to the conventional annular one. In this study, we investigated two thruster configurations, namely, cylindrical with the dimensions specified above, and annular with the same channel outer and inner diameters, and length. The overall diameter and the thruster length are both 7 cm.

Two electromagnetic coils are connected to separate power supplies. The currents in the coils are codirected in the conventional configuration and counterdirected in the cylindrical configuration to produce cusp magnetic field with a strong radial component in the channel. Figure 2 shows results of simulations of the magnetic field distribution for the annular and cylindrical thrusters. The magnetic field was measured inside both these thrusters with a miniature Hall probe with dimensions 1.5 mm × 1.5 mm. The results of

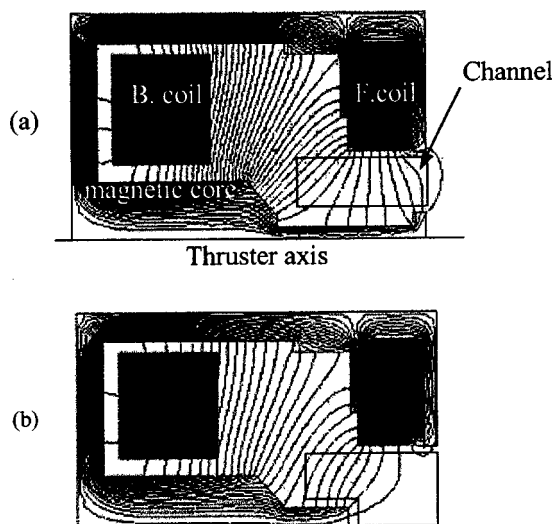


FIG. 2. Magnetic circuit and magnetic field distribution for the annular (a) and the cylindrical (b) thrusters. The channel outer diameter is 2.6 cm.

these measurements and simulations are in a good agreement.

For example, for the operating currents of 1.4 A in the back coil and 0.9 A in the front coil, the maximum radial magnetic field is 400 G at the inner wall near the exit of the annular channel. In the cylindrical configuration, the radial magnetic field reaches its maximum, which is about 700 G, a few millimeters from the anode near the inner wall of the short annular part and then reduces towards the thruster exit.

The experiments were carried out in a 0.4 m<sup>3</sup> vacuum chamber, equipped with a turbomolecular pumping system [Princeton Plasma Physics Laboratory (PPPL) Small Hall Thruster facility]. The measured pumping speed reached  $\sim 1700 \pm 300$  1/s for Xe. The working background pressure of Xe was about  $7 \times 10^{-5}$  Torr for the total propellant flow rate of 0.8 mg/s. Uncertainty in the determining of the pumping speed was caused by discrepancies in the readings of two Bayard-Alpert tabulated ion gauges used to measure the background pressure. Two commercial flow controllers, 0–10 sccm and 0–15 sccm, volumetrically calibrated in the flow rate range of 1–10 sccm, supplied research grade Xe gas to the anode and the cathode, respectively. A commercial HeatWave plasma source was used as a cathode neutralizer. The cathode flow rate of Xe was held at 0.2 mg/s for all the experiments.

The total ion flux coming from the thruster and the plume angle were measured by a movable electrostatic graphite probe with a guarding sleeve. Graphite was chosen as a probe material because of its extremely low sputtering coefficient for Xe ions with energies lower than or about 500 eV. The probe could be rotated in the vertical plane  $\pm 90^\circ$  relative to the thruster exit. The probe collecting surface always points at the thruster center. The distance between the probe and the thruster center is 14 cm. Yet, another probe mounted on the same movable arm was used to measure the flux of backstreaming ions. The second probe is horizontally shifted about 2 cm away from the first one, and its collecting surface points out from the thruster.

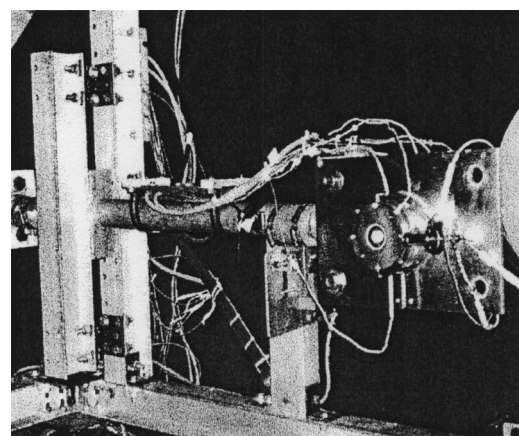


FIG. 3. 2.6 cm annular Hall thruster mounted on the thrust stand.

Thrust measurements were performed in the Electric Propulsion and Plasma Dynamics Laboratory (EPPDL) at Princeton University. The EPPDL thrust stand<sup>13</sup> was designed to accurately measure impulse bits for pulsed plasma thrusters (PPTs) within the range of  $10^{-4}$ –10 Ns. However, it was also predicted to be capable of measuring low steady-state thrust, as low as 20  $\mu$ N.

The thruster was mounted on a swinging arm thrust stand.<sup>14</sup> Figure 3 shows the 2.6 cm annular Hall thruster attached to the arm. The thrust arm was mounted with two flexural pivots. Thrust arm displacement from the equilibrium position was measured by a linear voltage differential transformer.

During steady-state thruster operation, the thrust is directly proportional to the displacement of the arm:

$$T = k_{\text{eff}}(x - x_{\text{equil}}), \quad (1)$$

where  $k_{\text{eff}}$  is the effective spring constant of the thrust stand. The effective spring constant is due to torsion exerted in the pivots, as well as restoring forces produced by the thruster wiring and the flexible silicon gas line (see Fig. 3), which connect the thruster with a fixed rigid part of the stand. In the present setup, it is impossible to eliminate the contribution of the wiring and the gas line to the effective spring constant. Although experimentally minimized, this contribution was of the order of the torsional spring constant of the flexural pivots.

It is worth mentioning that, for the same discharge voltage, coil currents, and propellant flows, the values of the discharge current measured at the EPPDL vacuum facility<sup>13</sup> were generally about 10% lower than those measured at the PPPL Small Hall Thruster facility. This apparently was due to the fact that the operating background pressure of Xe (about  $1 \times 10^{-5}$  Torr for the total propellant flow rate of 0.8 mg/s) was typically five to seven times lower than that at the PPPL facility.

### III. EXPERIMENTAL RESULTS AND DISCUSSION

#### A. Ion current and voltage-current characteristics

The 2.6 cm Hall thruster was operated at the discharge voltages of 150–300 V and Xe mass flow rates of 0.4–0.8

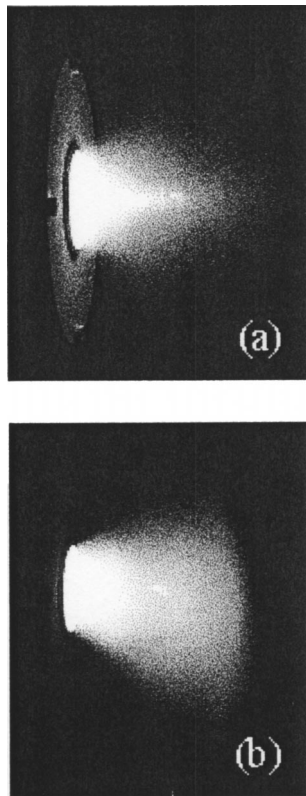


FIG. 4. Thruster operation in the annular (a) and cylindrical (b) configurations.

mg/s. The cathode was placed close to the thruster exit at the  $30^\circ$  angle to the thruster axis (Fig. 1). Thruster operation in the cylindrical and annular configurations is shown in Fig. 4.

Illustrative curves of voltage–current characteristics measured for each thruster configuration are shown in Fig. 5(a). At given discharge voltage and propellant flow rate, the discharge current, and, consequently, the input power in the cylindrical thruster, are both larger than those in the annular thruster by factor of 1.5–2. However, the current utilization efficiency, which is the ratio of the ion current at the exit plane of the thruster to the total discharge current, differs on average by about 10% only at voltages of 250–300 V [Fig. 5(b)]. The reason for this is an exceptionally high propellant ionization efficiency of the cylindrical thruster.

The thruster ionization efficiency is characterized by a so-called propellant utilization coefficient  $\eta_I$  — a ratio of the total ion current  $I_i$  at the thruster exit plane to the propellant flow rate  $\mu$  measured in units of electric current. Namely,  $\eta_I = I_i M / e \mu$ , where  $M$  is a mass of a propellant gas atom and  $e$  is the electron charge. In Fig. 6,  $\eta_I$  is plotted versus discharge voltage for the cylindrical and annular configurations. Propellant utilization for the cylindrical configuration can be seen to be much higher than that for the annular one. It increases with the discharge voltage and exceeds unity at high voltages, which implies a presence of Xe ions in charge states higher than +1 in the ion flux.

The increase in propellant utilization in the cylindrical configuration might be explained by ionization enhancement due to an increase in the electron density. As seen from Fig. 5(b), the electron current to the anode in the cylindrical

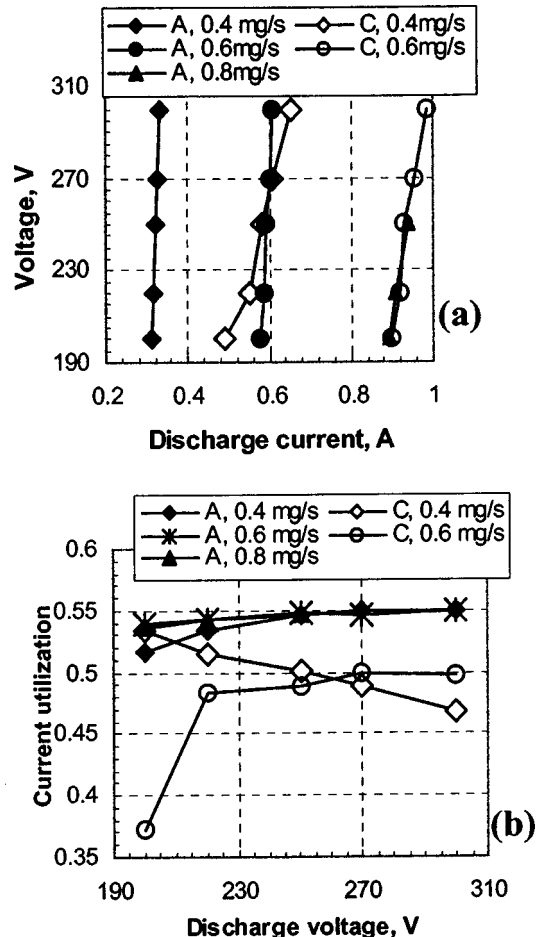


FIG. 5. (a) Discharge voltage vs current characteristics for the 2.6 cm cylindrical (C) and annular (A) thrusters (as measured at the PPPL experimental facility). The cathode flow rate is 0.2 mg/s. (b) Ratio of the ion current at the exit of the thruster to the discharge current vs the discharge voltage.

thruster is larger than in the annular. On the other hand, the electron mobility across the magnetic field must be lower in the cylindrical configuration, because the radial component of the magnetic field is typically 1.5–2 times larger than that in the annular one. Therefore, the electron density in the

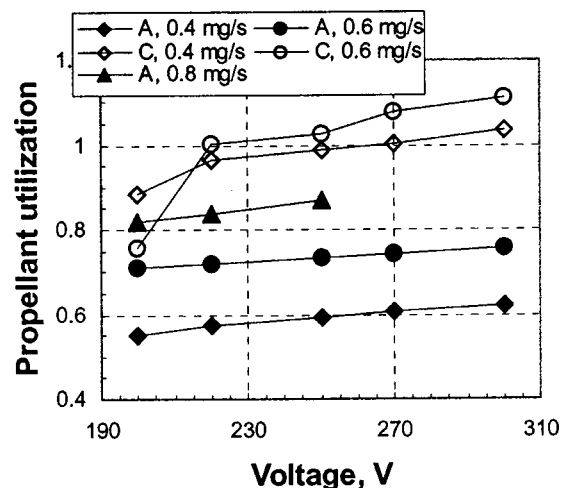


FIG. 6. Propellant utilization coefficient vs discharge voltage for the 2.6 cm cylindrical (C) and annular (A) thrusters.

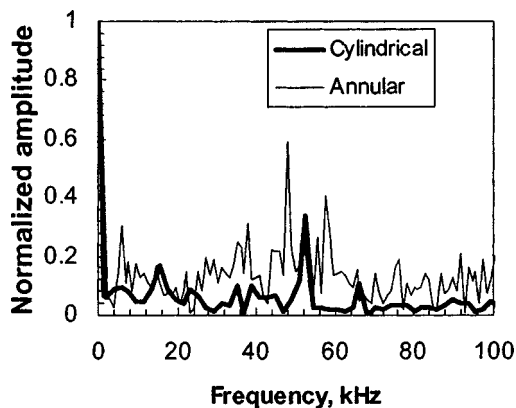


FIG. 7. Spectra of discharge current oscillations for the annular and cylindrical thrusters at  $U_d = 300$  V and anode flow rate of 0.4 mg/s.

channel is expected to be higher in the cylindrical configuration. Simple estimates show that a 25% increase in the propellant utilization (see Fig. 6) requires only about two-fold increase in the electron density. However, an increase in the radial magnetic field in a conventional annular thruster does not lead to a corresponding increase in the electron density because of the onset of strong high-frequency discharge current oscillations.<sup>11</sup>

The fact that the ion flux produced by the thruster can contain a substantial portion of multiply charged Xe ions is of particular interest. It is worth mentioning that even in conventional Hall thrusters, where the propellant utilization coefficient is typically 0.8–0.9, an ion flux can have rather large fractions of  $\text{Xe}^{2+}$  and  $\text{Xe}^{3+}$  ions.<sup>15</sup> The major factor in multicharged ion formation in a Hall thruster is the ion residence time in the channel. Simple estimates show that the time of flight of a  $\text{Xe}^+$  ion through a channel is much smaller than the time of ionization to higher charge states. Indeed, one expects a plasma in a miniaturized Hall thruster to have electron density of about  $10^{12} \text{ cm}^{-3}$  and electron temperature of 10–20 eV.<sup>16</sup> For example, for  $T_e \sim 20$  eV, the rate coefficient for single-electron impact ionization  $\text{Xe}^{+1} \rightarrow \text{Xe}^{+2}$  is about  $k_{1,2} \sim 4 \times 10^{-8} \text{ cm}^3/\text{s}$ .<sup>17</sup> Therefore, even for a moderately energetic ion with  $E_i = 50$  eV, the time of flight through a channel with length  $L = 3$  cm  $\tau_f \sim L/V_i \sim 4 \times 10^{-6}$  s is approximately an order of magnitude smaller than the ionization time  $\tau_{1,2} \sim (n_e k_{1,2})^{-1} \sim 3 \times 10^{-5}$  s. Thus, in this regime, we expect the number of ionization events to scale linearly with the residue time. The presence of a significant number of multicharged ions in the outgoing ion flux might be an indication of complex ion dynamics (possibly, non-straight trajectories, trapping by ambipolar potential, etc.), which increase the ion life time inside the channel. The formation of an ion charge state distribution in a Hall thruster discharge is worth studying further.

## B. Discharge oscillations

Typical spectra of the discharge current oscillations are shown in Fig. 7. Although the amplitude of oscillations is relatively lower for the cylindrical configuration, the discharge at low propellant flow rates is not as quiet as it was found to be in the large 9 cm cylindrical thruster.<sup>10</sup> The char-

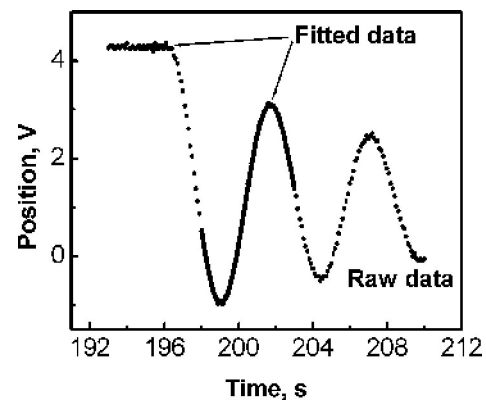


FIG. 8. An exemplary trace of thrust arm position vs time. At  $t \approx 196.3$  s, the thruster was turned off. Time interval from 198 to 203 s is used for curve fitting with a damped linear oscillator response function (solid line) to determine the instantaneous equilibrium position. A two-second interval (solid line) before the turning off is used to determine the arm displacement caused by the produced thrust.

acteristic peak at frequencies 50–60 kHz may be due to the ionization instability, which appears because of the depletion of neutral atoms in the ionization and acceleration regions.<sup>11</sup> The characteristic frequency of these oscillations scales as  $f \sim v_n/L_i$ , where  $v_n$  is the thermal speed of neutral atoms and  $L_i$  is the ionization region length. Apparently, the characteristic frequency, which was typically about 20 kHz for a 9 cm annular Hall thruster,<sup>10</sup> almost triples as  $L_i$ , together with the thruster sizes, are reduced by factor of about 3.

## C. Thrust and efficiency

As mentioned herein, the thrust stand had not been specifically designed to suit the experimental environment of a steady-state Hall thruster operation. Thruster operation showed that the heat generated by the thruster brought about a weak long-timescale thermal drift of the thrust stand equilibrium position. The larger the thruster operating power, the more visible this effect. However, it was experimentally found that the thrust stand moment of inertia remained almost unaffected by a temperature change due to the thruster operation.

In order to minimize the uncertainty of the thrust measurements caused by the equilibrium position drift, a procedure to determine an “instantaneous” equilibrium position and  $k_{\text{eff}}$ , was developed. Once the steady-state operation of the thruster was achieved (about 20 min from the ignition of the discharge), the discharge voltage, the coil power, and the gas flow to the anode and cathode were turned off, and oscillations of the thrust arm position  $x(t)$  were recorded (Fig. 8).

The thrust arm position  $x_0$  corresponding to the firing thruster was determined from averaging  $x(t)$  over a two-second interval immediately before turning the thruster off. The instantaneous equilibrium position  $x_{\text{equil}}$  together with  $k_{\text{eff}}$  were determined from fitting approximately half of the oscillations period right after the turning off with a damped linear oscillator response function.<sup>13</sup> The thrust was calculated then according to Eq. (1). For each set of operating parameters, the thrust measurement was repeated several

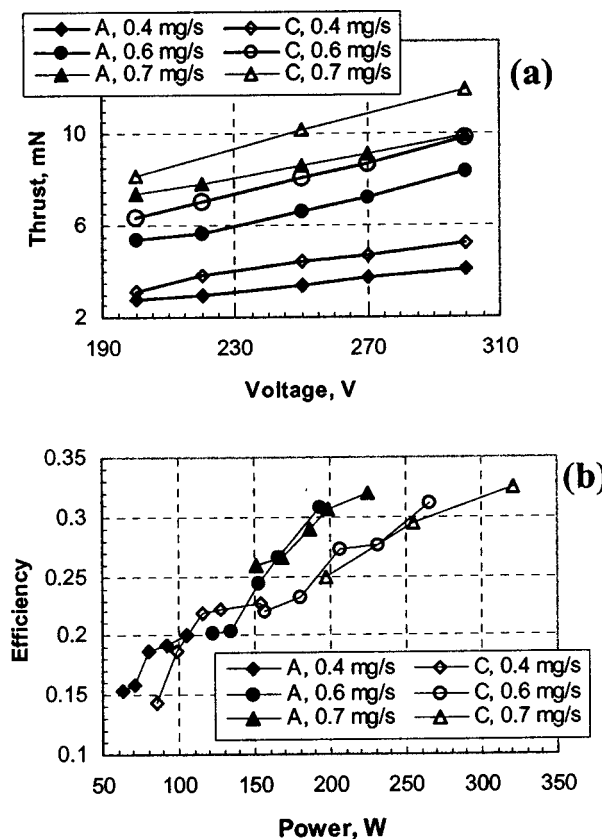


FIG. 9. (a) Measured thrust vs discharge voltage and (b) efficiency as a function of input power for different anode flow rates for the 2.6 cm cylindrical (C) and annular (A) thrusters. The estimated error bars on thrust and efficiency are  $\pm 3\%$  and  $\pm 6\%$ , respectively, for all regimes except for the case of cylindrical configuration with anode flow rate of 0.7 mg/s, where the error bars are  $\pm 6\%$  for thrust and  $\pm 12\%$  for efficiency.

times to minimize the statistical error. This measurement procedure ensured good repeatability of results.

Figure 9 shows measured thrust versus discharge voltage and efficiency versus input power for different anode flow rates for the cylindrical and annular configurations of 2.6 cm Hall thruster. In all regimes but one, the estimated error bars on thrust and efficiency are  $\pm 3\%$  and  $\pm 6\%$ , respectively, which is comparable with typical values of errors for most of the low-thrust measurements.<sup>6,7</sup> In the case of cylindrical configuration with anode flow rate of 0.7 mg/s, the error bars are  $\pm 6\%$  for thrust and  $\pm 12\%$  for efficiency. These relatively larger measurement errors are due to the more pronounced thrust stand thermal drift, observed at high operating power, and, partly, to the anode unstable operation in this particular regime. Anode unstable operation was supposedly caused by the anode overheating.

Measured thrust ranges from about 3 mN (200 V and 86 W) to 12 mN (300 V and 320 W) for the cylindrical configuration, and from about 2.5 mN (200 V and 63 W) to 10 mN (300 V and 225 W) for the annular configuration. For any given discharge voltage and anode flow rate in the range of parameters investigated, the thrust generated in the cylindrical configuration is larger than that in the annular configuration. This is another indication that the cylindrical configu-

ration has a better propellant ionization capability (see Fig. 6).

It is worth mentioning that the cylindrical thruster can be operated at the discharge voltage lower than 200 V, while for the annular configuration such voltage is not sufficient to sustain the discharge at low propellant flow rates. In Fig. 9, the voltage is kept at least at 200 V only in order to make a comparison between the two configurations.

The average ion exhaust velocity, defined as the ratio of the thrust to the anode propellant flow rate  $V_{ex} = T/\mu$ , ranges from 7 km/s ( $\mu = 0.4$  mg/s and  $U_d = 200$  V) to 14.5 km/s ( $\mu = 0.7$  mg/s and  $U_d = 300$  V) for the annular configuration, and from 8 km/s ( $\mu = 0.4$  mg/s and  $U_d = 200$  V) to 17.4 km/s ( $\mu = 0.7$  mg/s and  $U_d = 300$  V) for the cylindrical configuration. The values of  $V_{ex}$  attainable with a 2.6 cm cylindrical thruster, in the power range above 250 W, even exceed those typical of moderate-sized conventional Hall thrusters (about 16 km/s).

The efficiency  $\eta$  was calculated, using the measured thrust  $T$ , flow rate  $\mu$  and power  $P$ , as  $\eta = T^2/2\mu P$ . The cathode power and propellant flow and the magnet losses were not taken into account. Therefore, the efficiency plotted in Fig. 9(b) is a so-called “anode” efficiency. As can be seen from the graphs in Fig. 9(b), the cylindrical and annular thrusters have comparable efficiencies. This, in principle, gives an opportunity to develop a low-power Hall thruster capable of generating a variable thrust at given efficiency and thruster power. The use of a variable-thrust thruster is required for optimization of a propellant expenditure on satellites.<sup>18</sup> Thrust variation can be achieved in the 2.6 cm Hall thruster by changing the length of the central magnetic pole and channel piece. At constant power, one can increase the thrust (and decrease the ion exhaust velocity) by converting the thruster from the cylindrical to the annular configuration. For example, at power of about 120 W [see Figs. 9(a) and 9(b)], the transition between  $\mu = 0.4$  mg/s and  $U_d = 250$  V in the cylindrical configuration and  $\mu = 0.6$  mg/s and  $U_d = 200$  V in the annular configuration decreases efficiency by less than 2%, while the increase in thrust is 21%.

#### IV. CONCLUSIONS

Annular conventional Hall thrusters become inefficient when scaled to small sizes because of the large surface-to-volume ratio and the difficulty in miniaturizing the magnetic circuit. An alternative approach, which may be more suitable for scaling to low power, is a cylindrical Hall thruster. A 2.6 cm miniaturized cylindrical Hall thruster was developed and operated in a broad range of operating parameters. Its performance was compared to that of a conventional annular thruster of the same dimensions. Several interesting effects were observed.

The ion flux and thrust measurements showed that propellant ionization efficiency of the cylindrical thruster is much higher than that of the annular. Therefore, gases or gas mixtures that are harder to ionize than Xe may be used as a propellant; for example, one can use argon to generate larger ion exhaust velocities. In the cylindrical thruster, at high propellant flow rates, a significant fraction of multicharged xe-

non ions can be present in the outgoing ion flux. This may indicate complex ion dynamics that increase the ion life time in the channel. The formation of multicharged ions in a cylindrical Hall thruster discharge, which can differ significantly from that in an annular thruster, is a subject of ongoing research.

Discharge characteristics of the cylindrical thruster are comparable to those measured for the annular thruster. Although relatively quiet operation of the cylindrical thruster was observed, the discharge at low propellant flows is not as quiet as it was found to be in the large 9 cm cylindrical thruster. The characteristic peak at frequencies 50–60 kHz may be due to the ionization instability, which frequency approximately triples as the thruster sizes are reduced by factor of 3.

At a given discharge voltage and propellant flow rate, the discharge current and input power of the cylindrical thruster are higher than those of the annular one. The higher power and current would tend to erode the thruster faster; on the other hand, the cylindrical thruster has a lower surface-to-volume ratio and fewer inner parts. The lifetime comparison, therefore, remains an open question.

In the power range 50–300 W, the cylindrical and annular thrusters have comparable efficiencies ( $\eta=15\%-32\%$ ) and thrusts ( $T=2.5-12\text{ mN}$ ). Since these configurations may be controlled electronically, it may be possible to develop an efficient low-power Hall thruster with a variable thrust.

The values of efficiency for both configurations are comparable to those of other currently existing Hall microthrusters. For example, BHT-200-X2B<sup>6</sup> has channel diameter  $d=2.1\text{ cm}$  and operates at power  $P=100-300\text{ W}$  with efficiency  $\eta=20\%-45\%$ , SPT-30<sup>7</sup> has  $d=3\text{ cm}$ ,  $P=100-260\text{ W}$ , and  $\eta=16\%-34\%$ .

For the annular configuration, a voltage less than 200 V was not sufficient to sustain the discharge at low propellant flow rates. However, the cylindrical thruster can operate at low voltages ( $U_d < 200\text{ V}$ ). Operation at low voltage is important for three reasons: (i) certain missions may require lower ion exhaust velocity, (ii) voltages lower than 200 V may be accommodated by direct drive power, which could enormously simplify the power processing unit on a small satellite, and (iii) the operation at low voltage implies that further miniaturization may be possible, thereby allowing even lower-power operation.

Finally, it is important to note that the operating conditions attained here for the cylindrical thruster have not been completely optimized. There is a considerable flexibility in the magnetic configuration, and that has not been fully addressed. Furthermore, there may be added flexibility in the use of segmented electrodes in order to impose a potential

profile, as was done in the case of the annular thruster.<sup>19,20</sup> Any further control of the electric-field profile in the cylindrical thruster is likely to allow enhanced performance, because the operation of this thruster is particularly sensitive to the location of the acceleration region, both radially and axially.

## ACKNOWLEDGMENTS

The authors would like to thank Professor Edgar Choueiri for the provided opportunity to work with the EPPDL thrust stand, Kurt Polzin for his assistance in the thrust measurements, and David Staack for help in the experiments at the PPPL facility. This work was supported by grants from AFOSR, DARPA, and U.S. DOE Contract No. AC02-76CH0-3073.

- <sup>1</sup>R. M. Jones, J. Br. Interplanet. Soc. **42**, 2588 (1989).
- <sup>2</sup>R. L. Ticker and D. McLennan, Proceedings of IEEE Aerospace Conference, Big Sky, MN, March 10–17, 2001.
- <sup>3</sup>J. Mueller, in *Micropropulsion for Small Spacecraft*, AIAA Progress in Astronautics and Aeronautics, edited by M.M. Micci and A.D. Ketsdever (AIAA, Reston, VA, 2000), Vol. 187, p. 45.
- <sup>4</sup>A. I. Morozov and V. V. Savel'yev, in *Review of Plasma Physics*, edited by B. B. Kadomtsev and V. D. Shafranov (Consultants Bureau, New York, 2000), Vol. 21, p. 203.
- <sup>5</sup>J. Ashkenazy, Y. Raitses, and G. Appelbaum, Proceedings of the Second International Spacecraft Propulsion Conference, Noordwijk, The Netherlands, May 27–29, 1997.
- <sup>6</sup>V. Hruby, J. Monheiser, B. Pote, C. Freeman, and W. Connolly, Proceedings of the 26th International Electric Propulsion Conference, Kitakyushu, Japan, October 17–21, 1999, IEPC paper 99-092.
- <sup>7</sup>D. Jacobson and R. Jankovsky, Proceedings of the 34th Joint Propulsion Conference, Cleveland, OH, July 13–15, 1998, AIAA paper 98-3792.
- <sup>8</sup>O. Gorshkov, Proceedings of the 34th Joint Propulsion Conference, Cleveland, OH, July 13–15, 1998, AIAA paper 98-3929.
- <sup>9</sup>V. Khayms and M. Martinez-Sánchez, in *Micropropulsion for Small Spacecraft*, Progress in Astronautics and Aeronautics, edited by M. M. Micci and A. D. Ketsdever (AIAA, Reston, VA, 2000), Vol. 187, p. 45.
- <sup>10</sup>Y. Raitses and N. J. Fisch, Phys. Plasmas **8**, 2579 (2001).
- <sup>11</sup>J. P. Boeuf and L. Garrigues, J. Appl. Phys. **84**, 3541 (1998).
- <sup>12</sup>A. Smirnov, Y. Raitses, and N. J. Fisch, Proceedings of the 27th International Electric Propulsion Conference, Pasadena, CA, October 15–19, 2001, IEPC paper 01-038.
- <sup>13</sup>E. A. Cubbin, J. K. Ziener, E. Y. Choueiri, and R. G. Jahn, Rev. Sci. Instrum. **68**, 2339 (1997).
- <sup>14</sup>Full description of the thrust stand, the calibration procedure, as well as the measurement procedure for PPTs are given in E. A. Cubbin, J. K. Ziener, E. Y. Choueiri, R. G. Jahn, Rev. Sci. Instrum. **68**, 2339 (1997). In the present paper, we describe the thrust stand features relevant to a steady-state Hall thruster operation only.
- <sup>15</sup>L. B. King and A. D. Gallimore, Proceedings of the 34th Joint Propulsion Conference, Cleveland, OH, July 13–15, 1998, AIAA paper 98-3641.
- <sup>16</sup>A. Bishaev and V. Kim, Sov. Phys. Tech. Phys. **23**, 1055 (1978).
- <sup>17</sup>E. W. Bell, N. Djuric, and G. H. Dunn, Phys. Rev. A **48**, 4286 (1993).
- <sup>18</sup>J. P. Marek, *Optimal Space Trajectories* (Elsevier, Amsterdam, 1979), pp. 7–19 and 38.
- <sup>19</sup>Y. Raitses, L. A. Dorf, A. A. Litvak, and N. J. Fisch, J. Appl. Phys. **88**, 1263 (2000).
- <sup>20</sup>N. J. Fisch, Y. Raitses, L. A. Dorf, and A. A. Litvak, J. Appl. Phys. **89**, 2040 (2001).